Coulomb excitation of ^{183}W

F. K. McGowan, C. E. Bemis, Jr., J. L. C. Ford, Jr., W. T. Milner, D. Shapira, and P. H. Stelson
Oak Ridge National Laboratory, Oak Ridge, Tennessee 37830
(Received 17 May 1979)

Direct $E2$ and multiple Coulomb excitation of states up to $J = 9/2$ in the $K = 1/2$ and $K = 3/2$ bands of ^{183}W has been measured by means of γ-ray spectroscopy. Excitation was produced by 15-MeV ^{4}He ions on a thick target of W with natural abundance. Excitation probabilities were also determined relative to the elastic scattering by the observation of the (α,α') reaction on ^{183}W with 13-MeV ^{4}He ions using a split-pole magnetic spectrometer equipped with a position-sensitive proportional detector. The $B(E2)$ values for excitation of the $3/2^L$, $5/2^L$, $3/2^H$, and $5/2^H$ states (H and L refer to the high and low energy states of the same total angular momentum J) are obtained and information is given on the reduced transition probabilities for the different decay modes of these states. In particular, the prediction of strong cancellation in the $E2$ transition probabilities for the $3/2^H \rightarrow 1/2^L$, $3/2^H \rightarrow 5/2^L$, and $5/2^H \rightarrow 5/2^L$ transitions from Coriolis interaction calculations has been verified by the experimental results. The experimental results are compared with several calculations of the Coriolis coupling between the rotational bands. Several weakly excited states between 0.9 and 1.5 MeV were observed and the $B(E2)$ for excitation of these states are $\leq B(E2)_{\text{s.p.}}$

[NUCLEAR REACTIONS ^{183}W$(\alpha,\alpha'\gamma)$, $E = 15$ MeV, ^{183}W(α,α'), $E = 13$ MeV; measured E_γ, I_γ, $\gamma(\theta)$, $\sigma(E_{\alpha'}; \theta = 150)$; ^{183}W levels deduced $B(E2)$, $B(M1)$, J^π, δ. Enriched target.]

I. INTRODUCTION

In many odd-A nuclei with deformed equilibrium shapes, the energy levels do not follow closely the $J(J+1)$ law for rotational bands. The energy levels and the transition probabilities of many of these nuclei are often better fitted by the rotational model if the decoupling effect of the Coriolis interaction[1] is taken into consideration. Close-lying bands whose K quantum numbers differ by unity may be strongly mixed by the Coriolis interaction (sometimes referred to as rotation-particle coupling). The nucleus ^{183}W is the classic example for such a band mixing effect. From the precise γ-ray energy measurements by Murray *et al.*,[2] Kerman[3] extracted the mixing amplitudes for the states in the $K = \frac{1}{2}$ and $K = \frac{3}{2}$ bands of ^{183}W which are shown in Fig. 1. With the mixing amplitudes and five additional parameters, Kerman calculated 20 $E2$ and $M1$ transition probabilities for the γ rays from decay of these states. The fits to the energy levels were excellent and his predictions for the relative γ-ray intensities were in fair agreement with the experimental intensities.[2]

Subsequently, the relative γ-ray intensities of the transitions in ^{183}W were measured with an accuracy of $\pm 5\%$.[4,5] Rowe[6] analyzed these data with the Coriolis coupling between rotational bands and included some $\Delta K = 2$ band-mixing effects of the type found in even-even nuclei. The data were fitted equally well but there seemed to be no real necessity to require the presence of any $\Delta K = 2$ band mixing to fit the relative γ-ray intensities. Brockmeier *et al.*[7] obtained an improvement in the fit to the energy levels when seven other Nilsson

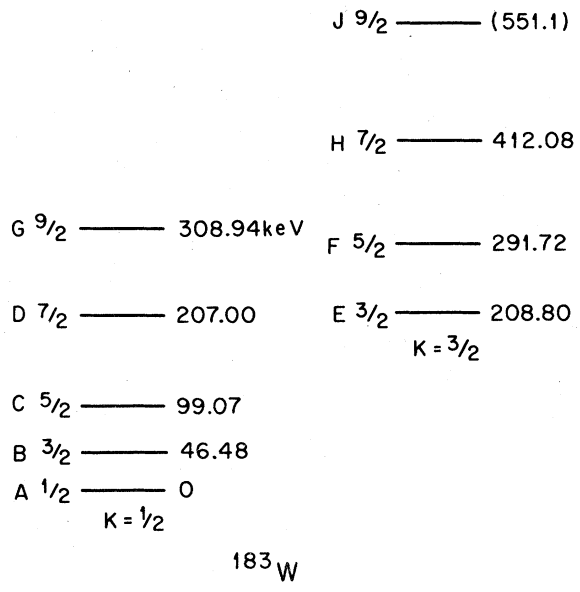

FIG. 1. The experimental energy levels of the $K = \frac{1}{2}$ and $K = \frac{3}{2}$ bands in ^{183}W.

states were also included in the analysis. On the other hand, the inclusion of the additional states in the Coriolis band-mixing analysis did not improve the γ-ray intensity fit compared to that from mixing only the $K=\frac{1}{2}$ and $\frac{3}{2}$ bands.

These two analyses by Rowe and Brockmeier *et al.* do differ, however, for several of the absolute transition probabilities. For example, Rowe neglected the off-diagonal matrix elements in the calculation of the $E2$ transition probabilities because these are of single-particle magnitude. Brockmeier *et al.*, however, calculated the $E2$ transition probabilities without simplifying assumptions. For instance, the calculations by Brockmeier *et al.* predict a strong cancellation in the $E2$ transition probabilities for the $\frac{3}{2}^H \rightarrow \frac{1}{2}^L$, $\frac{5}{2}^H \rightarrow \frac{3}{2}^L$, and $\frac{5}{2}^H \rightarrow \frac{5}{2}^L$ transitions (H and L refer to the high and low energy states of the some total angular momentum J).

The single-nucleon-transfer reactions on even-even target nuclei provide a powerful technique for identifying Nilsson single-particle states in odd-A nuclei. The differential cross section for exciting a particular rotational-band member is expected to be proportional to the square of a single C_{jl}^K expansion coefficient. Since each Nilsson state is characterized by an unique set of expansion coefficients, the single-nucleon-transfer cross sections into the successive members of a rotational band should exhibit a distinctive pattern. There are, however, deviations from this simple Nilsson scheme in many odd-A nuclei. For instance, Casten *et al.*[20] found that many of the discrepancies between the experimental cross sections and the calculated cross sections using the Nilsson model could be eliminated by the inclusion of the Coriolis interaction for the odd-A tungsten nuclei. This mixing of Nilsson states alters energies of the states as well as cross sections.

The amplitudes of the mixed wave functions obtained by fitting the excitation energies from a Coriolis coupling calculation by Casten *et al.* improved the agreement between calculated and experimental cross sections for the $\frac{1}{2}^-[510]$ and $\frac{3}{2}^-[512]$ bands in ^{183}W. Seven Nilsson states were included in the analysis. The signs of the mixing amplitudes for the $K=\frac{1}{2}^-$ and $K=\frac{3}{2}^-$ components correspond to a negative value and smaller magnitude for the parameter $A_{1/2}$ (Brockmeier *et al.* notation) entering in the Coriolis matrix element between the main components $K=\frac{1}{2}^-$ and $K=\frac{3}{2}^-$. On the one hand, Brockmeier *et al.* found the best energy fit with $A_{1/2}>0$ and also found that the γ-ray intensity fits with $A_{1/2}<0$ were much poorer. On the other hand, results from the single-nucleon-transfer reactions tend to give more direct evidence on the wave functions of the observed bands. Therefore, measurements of the absolute transition probabilities would provide a good test of the wave functions used in the calculations. In this paper, we present results from the Coulomb excitation reactions $(\alpha,\alpha'\gamma)$ and (α,α').

II. EXPERIMENTAL METHOD

A. Gamma-ray spectroscopy

The γ-ray yields were measured with 15-MeV ^{4}He ions incident on a thick target of W with natural abundance. Gamma-ray spectra were observed at $\theta_\gamma=0°$, 55°, and 90° with respect to the beam direction with a 60-cm^3 Ge(Li) detector located at 10 cm from the target. An example of a section from a 8192-channel γ-ray spectrum is shown in Fig. 2. Above each peak are given the energy of the γ ray in keV and the transition assignment. The weak γ rays at 259.4 and 344.1 keV are given the assignment $\frac{9}{2}^H \rightarrow \frac{5}{2}^H$ and $\frac{9}{2}^H \rightarrow \frac{7}{2}^L$, which means level J of Fig. 1 has the energy 551.1 keV. This position is 3.2 keV lower than previous assignments, viz., 554.3 keV if the 142.25-keV line[4] was assigned to the $\frac{9}{2}^H \rightarrow \frac{7}{2}^H$ transition. A weak γ ray at 452.0 keV in another section of our spectra is assigned to the $\frac{9}{2}^H \rightarrow \frac{5}{2}^L$ transition. Many of the contaminant γ rays are identified in Fig. 2. Those due to the ^{56}Fe$(\alpha,n)^{59}$Ni result from target impurity which undoubtedly was introduced by the rolling technique to produce the W foils. Other sections of the spectra contained additional γ rays from decay of states in ^{182,184,186}W (Ref. 8) and ^{183}W.

A summary of the γ-ray yields from decay of states in ^{183}W is presented in Table I. The last column also lists the anisotropies $R \equiv$ W(0°)/W(90°) from the γ-ray angular distributions. For the conditions of these experiments, the use of the first-order treatment of the Coulomb excitation process is adequate for the analysis of thick-target γ-ray yields from direct excitation of states with $J=\frac{3}{2}$ and $\frac{5}{2}$. The procedure needed to extract $B(E2)$ values from thick-target γ-ray yields has been described previously.[9,10] The remaining states either are excited by multiple Coulomb excitation or are populated by the γ-ray decay of the excited states. For instance, the γ-ray yields in Table I for the 160.5-, 162.3-, and 208.8-keV γ rays are gross yields. The peak areas for these γ rays contain contributions from decay of the directly excited $\frac{5}{2}^H$ state, viz., $\frac{5}{2}^H \rightarrow \frac{3}{2}^H$ and $\frac{5}{2}^H \rightarrow \frac{7}{2}^L$ (see Fig. 1). Because of this complication in the γ-ray spectroscopy, we made measurements of the (α,α') reaction to obtain a more direct measurement of excitation of the $\frac{3}{2}^H$ state at 208.8 keV.

B. Particle spectroscopy

Elastically and inelastically scattered ^{4}He ions at $\theta_{\rm lab}=150°$ and 90° from a 10 μg/cm^2 isotopically

TABLE I. Summary of γ-ray yields from the decay of states in ^{183}W. The column headed "yield" denotes the thick-target yield in gammas/nC (6.24×10^9 ions).

Initial state J^π	Initial state energy (keV)	Final state J^π	Final state energy (keV)	E (keV)	Yield (γ/nC)	W(0°)/W(90°)
$\frac{3}{2}^{H-}$	208.8	$\frac{3}{2}^{L-}$	46.5	162.3	485	1.12 ± 0.01
		$\frac{1}{2}^{L-}$	0.0	208.8	83	0.875 ± 0.016
$\frac{5}{2}^{H-}$	291.7	$\frac{5}{2}^{L-}$	99.1	192.6	118	1.220 ± 0.018
		$\frac{3}{2}^{L-}$	46.5	245.2	124	0.982 ± 0.021
		$\frac{1}{2}^{L-}$	0.0	291.7	1391	1.171 ± 0.012
$\frac{7}{2}^{L-}$	207.0	$\frac{3}{2}^{L-}$	46.5	160.5	164	1.15 ± 0.02
$\frac{9}{2}^{L-}$	308.9	$\frac{5}{2}^{L-}$	99.1	209.9	85	1.44 ± 0.03
$\frac{7}{2}^{H-}$	412.1	$\frac{5}{2}^{L-}$	99.1	313.0	14	
$\frac{9}{2}^{H-}$	551.1	$\frac{5}{2}^{H-}$	291.7	259.4	8.3	
		$\frac{7}{2}^{L-}$	207.0	344.1	4.7	
		$\frac{5}{2}^{L-}$	99.1	452.0	4.5	
$\frac{5}{2}^{-}$	903.5	$\frac{5}{2}^{L-}$	99.1	804.4	8.0	
		$\frac{3}{2}^{L-}$	46.5	857.0	7.4	
$\frac{3}{2}^{-}$	1026.3	$\frac{3}{2}^{L-}$	46.5	979.8	1.5	
		$\frac{1}{2}^{L-}$	0.0	1026.3	3.3	
$\frac{5}{2}^{-}$	1052.9	$\frac{7}{2}^{H-}$	412.1	640.8	≤1.0	
$\frac{3}{2}^{-}$	1149.8	$\frac{7}{2}^{L-}$	207.0	942.8	0.8	
		$\frac{1}{2}^{L-}$	0.0	1149.8	3.0	
$\frac{3}{2}^{-}$	1291.6	$\frac{5}{2}^{L-}$	99.1	1192.5	5.9	
		$\frac{1}{2}^{L-}$	0.0	1291.6	5.1	
$\frac{3}{2}^{-}$	1309.9	$\frac{3}{2}^{L-}$	46.5	1263.4	3.3	
		$\frac{1}{2}^{L-}$	0.0	1309.9	17	
$\frac{3}{2}^{-}$	1463.1	$\frac{7}{2}^{H-}$	412.1	1051.0	5.9	
$\frac{3}{2}^{-}$	1485.0	$\frac{5}{2}^{-}$	903.5	581.5	3.0	
		$\frac{3}{2}^{L-}$	46.5	1438.5	13	
		$\frac{1}{2}^{L-}$	0.0	1485.0	14	
$\frac{3}{2}^{-}$	1510.4	$\frac{7}{2}^{H-}$	412.1	1098.3	6.5	
		$\frac{3}{2}^{H-}$	208.8	1301.6	2.2	
$\frac{3}{2}^{-}$	1556.4	$\frac{5}{2}^{-}$	903.5	652.9	21	
		$\frac{7}{2}^{H-}$	412.1	1144.3	2.0	
		$\frac{3}{2}^{H-}$	208.8	1347.6	4.2	

pure target of ^{183}W on carbon backing (20 μg/cm^2) were observed at the focal plane of an Enge split-pole spectrometer at the EN tandem Van de Graaff by a 20-cm-long position-sensitive gas proportional detector. The target was prepared using a 150-cm radius 90° sector electromagnetic isotope separator as described previously.[11] Calibration of the Enge spectrometer and detector system have been discussed in an earlier communication.[11]

Figure 3 shows the spectrum of 13-MeV ^{4}He ions scattered from ^{183}W at a lab angle of 150°.

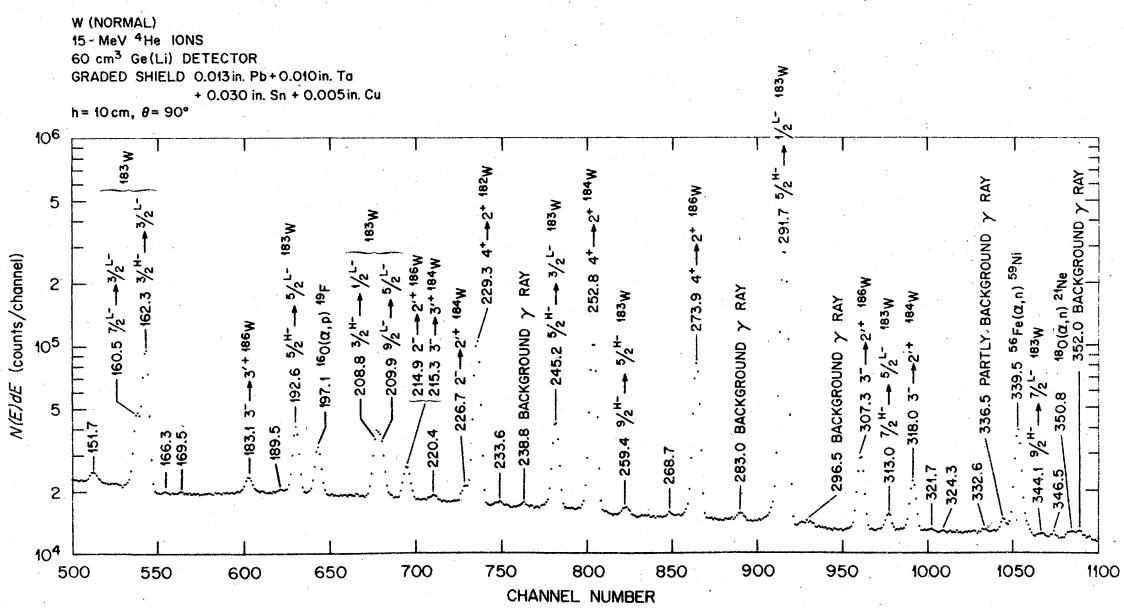

FIG. 2. A section from a 8192-channel pulse-height spectrum of the γ rays from a normal tungsten target bombarded with 15.0-MeV ^{4}He ions.

The energy resolution is 11 keV full width at half maximum which is more than adequate to separate the ground band rotational states $\frac{1}{2}L$, $\frac{3}{2}L$, and $\frac{5}{2}L$. The excitation probabilities for the $\frac{3}{2}L$, $\frac{5}{2}L$, $\frac{3}{2}H$, and $\frac{5}{2}H$ states were determined relative to the elastic scattering by integration of the appropriate peak areas.

III. EXPERIMENTAL RESULTS AND DISCUSSION

The experimental results for the reduced transition probabilities $B(E2, \frac{1}{2} \rightarrow J)$ are summarized in Table II. The K, J^π assignments were deduced from our $\gamma(\theta)$ measurements and results from other nuclear spectroscopy studies which have

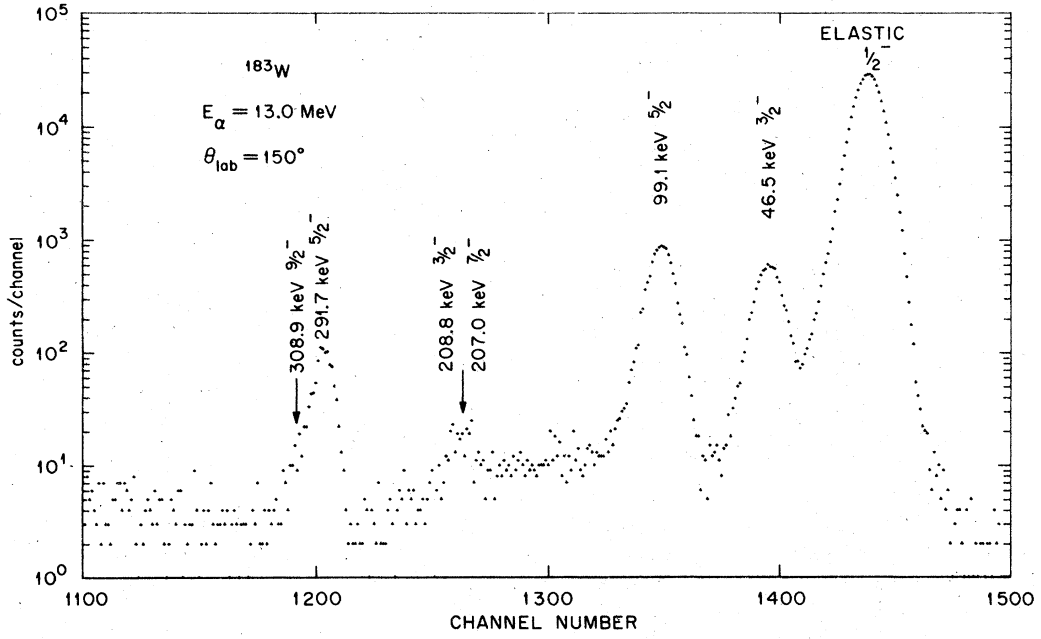

FIG. 3. Elastically and inelastically scattered 13.0-MeV ^{4}He ions from ^{183}W at a lab angle of 150°.

TABLE II. Measured $B(E2, \frac{1}{2} \rightarrow J)$ for excitation of states in ^{183}W. Unless noted by footnote, the results are from the γ-ray spectroscopy measurements.

Level (keV)	K, J^π	$B(E2, \frac{1}{2} \rightarrow J)$ $(e^2 \cdot b^2)$	$B(E2)\downarrow/B(E2)_{s.p.}$ [a]
46.5	$\frac{1}{2}, \frac{3}{2}^-$	1.63 ± 0.04 [b]	132
99.1	$\frac{1}{2}, \frac{5}{2}^-$	2.21 ± 0.03 [b]	119
208.8	$\frac{3}{2}, \frac{3}{2}^-$	$(1.5 \pm 0.5) \times 10^{-2}$ [b]	1.2
		$(0.62 \pm 0.43) \times 10^{-2}$	0.5
291.7	$\frac{3}{2}, \frac{5}{2}^-$	$(2.39 \pm 0.09) \times 10^{-1}$ [b]	12.9
		$(2.65 \pm 0.22) \times 10^{-1}$	14.3
903.5	$\frac{5}{2}, \frac{5}{2}^-$	$(6.4 \pm 0.6) \times 10^{-3}$	0.34
1026.3	$\frac{1}{2}, \frac{3}{2}^-$	$(1.0 \pm 0.2) \times 10^{-3}$	0.08
1052.9	$\frac{1}{2}, \frac{5}{2}^-$	$\leq 1.9 \times 10^{-3}$	≤ 0.10
1149.8	$\frac{3}{2}^-$	$(9.3 \pm 3.7) \times 10^{-4}$	0.08
1291.6	$\frac{3}{2}^-$	$(4.4 \pm 0.6) \times 10^{-3}$	0.35
1309.9	$\frac{3}{2}^-$	$(7.7 \pm 0.6) \times 10^{-3}$	0.62
1463.1	$\frac{3}{2}^-$	$(3.4 \pm 0.4) \times 10^{-3}$	0.27
1485.0	$\frac{3}{2}^-$	$(1.8 \pm 0.2) \times 10^{-2}$	1.5
1510.4	$\frac{3}{2}^-$	$(5.6 \pm 0.7) \times 10^{-3}$	0.45
1556.4	$\frac{3}{2}^-$	$(2.0 \pm 0.2) \times 10^{-2}$	1.6

[a] $B(\lambda)_{s.p.} = (1/4\pi)(3/\lambda + 3)^2 \ (0.12A^{1/3})^{2\lambda} e^2 b^\lambda$.
[b] From particle-spectroscopy measurements.

been summarized recently for $A = 183$.[12]

The experimental excitation probabilities from the particle-spectroscopy measurements were analyzed using the semiclassical $E2$ coupled-channels code of Winther and de Boer.[13] The nine states in Fig. 1 were included in the calculations of the Coulomb-excitation cross sections. The starting matrix elements, based on the mixing amplitudes $Z = 0$ (Kerman's solution) by Rowe,[6] included all possible reduced $E2$ matrix elements in the rigid-rotor limit which connect these states. In the case of the interband $E2$ matrix elements for decay of the $\frac{5}{2}^H$ and $\frac{3}{2}^H$ states, the experimental values of $B(E2, \frac{1}{2}^L \rightarrow \frac{5}{2}^H)$, $B(E2, \frac{1}{2}^L \rightarrow \frac{3}{2}^H)$, branching ratios, and $E2/M1$ ratios were available from the analyses of γ-ray spectroscopy of the Coulomb-excitation reaction and these were used in the calculations. The matrix elements $M_{1/2L3/2L}(E2)$, $M_{1/2L5/2L}(E2)$, $M_{1/2L3/2H}(E2)$, and $M_{1/2L5/2H}(E2)$ were then varied in an iteration procedure to produce the measured excitation probabilities. Half of the intensity of the composite peak from excitation of the $\frac{7}{2}^L$ and $\frac{3}{2}^H$ states at 207.0 and 208.8 keV in Fig. 3 is due to multiple Coulomb excitation of the $\frac{7}{2}^L$ state. The particle spectrum observed at 90° should have provided a more direct measurement of $B(E2, \frac{1}{2}^L \rightarrow \frac{3}{2}^H)$ because multiple excitation of the $\frac{7}{2}^L$ state contributes only 15% to the composite peak intensity. However, this advantage was more than offset by the higher background observed in the 90° spectrum. For excitation of the $\frac{5}{2}^H$ state at 291.7 keV, the multiple excitation of the $\frac{9}{2}^L$ state contributed only 7.1% and 2.6% to the composite peak intensity at $\theta_{lab} = 150°$ and 90°, respectively.

A. $\frac{3}{2}^L$ and $\frac{5}{2}^L$ states

The $B(E2)$ values for excitation of the $\frac{3}{2}^L$ and $\frac{5}{2}^L$ members of the $K = \frac{1}{2}$ rotational band are in good agreement with measurements from other Coulomb-excitation experiments,[14,15] viz.,

$$B(E2, \tfrac{1}{2}^L \rightarrow \tfrac{3}{2}^L) = 1.52 \pm 0.07 \text{ and } 1.50^{+0.16}_{-0.12} e^2 \cdot b^2$$

and

$$B(E2, \tfrac{1}{2}^L \rightarrow \tfrac{5}{2}^L) = 2.04 \pm 0.08 \text{ and } 2.31 \pm 0.11 e^2 \cdot b^2.$$

In Table III we give the $B(E2)$ and $B(M1)$ values for transitions between excited states based on our $B(E2)$ values for excitation of states in ^{183}W, adopted[12] photon intensities, and recommended[16] $E2/M1$ mixing ratios

$$\delta = \langle J_f \| E2 \| J_i \rangle / \langle J_f \| M1 \| J_i \rangle.$$

The photon intensities are based primarily on measurements[4,5] from ^{183}Ta decay and most of the $E2/M1$ mixing ratios are from measurements

by Krane *et al.*[17] The $B(E2)$ and $B(M1)$ obtained from the calculated absolute transition probabilities by Brockmeier *et al.*[7] and by Rowe[6] are also given in Table III. Fit $B(I)$ corresponds to mixing only the single-particle levels $K=\frac{1}{2}$ and $\frac{3}{2}$ whereas fit $B(II)$ includes seven additional Nilsson states in the analysis of Coriolis coupling between rotational bands. The fit $Z=0$ by Rowe corresponds to Kerman's solution, viz., mixing only of the close-lying levels $K=\frac{1}{2}$ and $\frac{3}{2}$ and neglecting the off-diagonal matrix elements for the $E2$ transition probabilities.

Utilizing the mixing amplitudes derived from fitting the energy of the states by Casten *et al.*,[20] we have calculated the reduced $E2$ transition probabilities from Eq. (21) of Brockmeier *et al.* retaining only the four dominant terms due to the $\frac{1}{2}^-[510]$ and $\frac{3}{2}^-[512]$ components, viz.,

$$B(E2;\nu,J\to\nu',J')=\frac{5e^2}{16\pi}\Big|\sum_{K,K'}C_{\nu'}(0,K';J')C_{\nu}(0,K;J)\,Q^{K',K}\times[(JK2,K'-K|J'K')+(-1)^{J'+K'}(JK2,-K'-K|J',-K')b_{E2}\times(\delta_{K,1/2}\delta_{K',3/2}+\delta_{K,3/2}\delta_{K',1/2})]\Big|^2.$$

The label ν refers to H and L the high and low energy states of the same J and the admixed amplitudes are $C_{\nu'}$ and C_{ν}. We fixed $Q^{1/2,1/2}=Q^{3/2,3/2}$ at $6.33b$ which is the average value of Q_0 deduced from the $B(E2,0\to2)$ for ^{182}W and ^{184}W. The off-diagonal matrix elements were adjusted to give the best overall fit to the $B(E2,\frac{3}{2}^H\to\frac{1}{2}^L)$ and $B(E2,\frac{5}{2}^H\to\frac{1}{2}^L)$, viz.,

$$Q^{1/2,3/2}=-Q^{3/2,1/2}=-0.019b \text{ and } b_{E2}=-56.$$

The results of these calculations are given in Table III. The argeement of these calculations with our reduced $E2$ transition probabilities for decay of the $\frac{3}{2}^L$ and $\frac{5}{2}^L$ states is slightly better than those from Brockmeier *et al.* and from Rowe.

B. $\frac{3}{2}^H$ and $\frac{5}{2}^H$ states

The $B(E2)$ values extracted from the γ-ray and the particle spectroscopy measurements for excitation of the $\frac{3}{2}^H$ and $\frac{5}{2}^H$ members of the $K=\frac{3}{2}$ rotational band are given in Table II. Only 13.6% of the gross γ-ray yields from the peaks at 162.3 and 208.8 keV is due to direct $E2$ excitation of the $\frac{3}{2}^H$ state. Our result for $B(E2,\frac{1}{2}^L\to\frac{3}{2}^H)$ is eight times smaller than the result from an early Coulomb-excitation measurement by Hansen *et al.*[14]

An additional test of our analysis of the γ-ray spectroscopy data comes from the angular distribution measurements of the 162.3- and 208.8 keV γ rays. These γ-ray distributions are composite angular distributions, viz., 1–3 correlation sequence

$$\tfrac{1}{2}^L(E2)\tfrac{5}{2}^H(E2+M1)\tfrac{3}{2}^H(E2+M1)\tfrac{3}{2}^L$$

plus a weak double correlation sequence $\frac{1}{2}^L(E2)\frac{3}{2}^H(E2+M1)\frac{3}{2}^L$ for the 162.3-keV transition and 1–3 correlation sequence

$$\tfrac{1}{2}^L(E2)\tfrac{5}{2}^H(E2+M1)\tfrac{3}{2}^H(E2+M1)\tfrac{1}{2}^L$$

plus a weak double correlation sequence $\frac{1}{2}^L(E2)\frac{3}{2}^H(E2+M1)\frac{1}{2}^L$ for the 208.8-keV transition. The expected values of the anisotropy R based on 13.6% of the gross γ-ray yields from direct $E2$ excitation and mixing ratios[17] $\delta(82.9\text{ keV})=0.63$, $\delta(162.3\text{ keV})=0.37$, and $\delta(208.8\text{ keV})=-0.30$ are $R=1.134$ and 0.873 for the 162.3 and 208.8 keV transitions, respectively. The agreement with $R_{\text{exp}}=1.12\pm0.01$ and 0.875 ± 0.016 from Table I is excellent.

The $B(E2)$ and $B(M1)$ values for transitions from decay of the $\frac{3}{2}^H$ and $\frac{5}{2}^H$ states and the values from the Coriolis coupling calculations are given in Table III. Aside from the $B(E2,\frac{5}{2}^H\to\frac{3}{2}^L)$, the agreement of the calculations, using the admixed amplitudes from Casten *et al.*, with our reduced $E2$ transition probabilities for decay of the $\frac{3}{2}^H$ and $\frac{5}{2}^H$ states is significantly better than the other calculations. The strong cancellations in the $E2$ transition probabilities predicted for the $\frac{3}{2}^H\to\frac{1}{2}^L$, $\frac{3}{2}^H\to\frac{5}{2}^L$, and $\frac{5}{2}^H\to\frac{5}{2}^L$ transitions are indeed verified by the experimental results. Although the general features of the $B(M1)$ values are reproduced by the calculations of Brockmeier *et al.* and Rowe, the experimental values of $B(M1)$ in most cases tend to be approximately a factor of 2 smaller than the predictions by Brockmeier *et al.* Eight of the nine relative phases for the $E2/M1$ mixtures (sign of δ) in Table III are in agreement with the predictions by Kerman.[3]

C. $\frac{7}{2}^L$, $\frac{9}{2}^L$, $\frac{7}{2}^H$, and $\frac{9}{2}^H$ states

The total yields for excitation of the $\frac{7}{2}^L$, $\frac{9}{2}^L$, and $\frac{7}{2}^H$ states were obtained from the γ-ray yields in Table I and the known branching ratios[12] for decay of these states. The total yield of the 160.5-keV transition $\frac{7}{2}^L\to\frac{3}{2}^L$ is consistent with feeding by the $\frac{5}{2}^H\to\frac{7}{2}^L$ transition plus the yield from multiple $E2$

TABLE III. Experimental and calculated $B(E2)$ and $B(M1)$ values for ^{183}W.

Transition $J_i \rightarrow J_f$	E_γ (keV)	I_γ	δ		$B(E2, J_i \rightarrow J_f)(e^2 \cdot b^2)$ Experiment	From Casten *et al.* Amplitudes	Brockmeier *et al.* Fit B(I)	Brockmeier *et al.* Fit B(II)	Rowe $Z=0$	$B(M1, J_i \rightarrow J_f)(nm^2)$ Experiment	Brockmeier *et al.* Fit B(I)	Rowe $Z=0$
$\frac{3}{2}^L \rightarrow \frac{1}{2}^L$	46.48	100	−0.061	6	$(8.15 \pm 0.20) \times 10^{-1}$	8.4×10^{-1}	7.5×10^{-1}	7.7×10^{-1}	7.6×10^{-1}	$(3.3 \pm 0.7) \times 10^{-1}$	2.8×10^{-1}	3.0×10^{-1}
$\frac{5}{2}^L \rightarrow \frac{1}{2}^L$	99.07	100	$E2$		$(7.37 \pm 0.10) \times 10^{-1}$	7.3×10^{-1}	7.0×10^{-1}	7.1×10^{-1}	7.5×10^{-1}			
$\frac{5}{2}^L \rightarrow \frac{3}{2}^L$	52.59	80	−0.13	2	$(2.3^{+0.8}_{-1.5}) \times 10^{-1}$	2.0×10^{-1}	2.2×10^{-1}	2.1×10^{-1}	3.0×10^{-1}	$(2.6 \pm 0.2) \times 10^{-2}$	3.2×10^{-2}	2.9×10^{-2}
$\frac{3}{2}^H \rightarrow \frac{1}{2}^L$	208.8	13	−0.34	4	$(5 \pm 2) \times 10^{-3}$	6.0×10^{-3}	0.17×10^{-3}	0.16×10^{-3}	48×10^{-3}	$(13.2 \pm 5.2) \times 10^{-4}$	26×10^{-4}	1.9×10^{-4}
$\frac{3}{2}^H \rightarrow \frac{3}{2}^L$	162.3	100	0.37	2	$(1.6 \pm 0.6) \times 10^{-1}$	2.2×10^{-1}	4.3×10^{-1}	3.9×10^{-1}	2.3×10^{-1}	$(2.1 \pm 0.8) \times 10^{-2}$	5.6×10^{-2}	5.9×10^{-2}
$\frac{3}{2}^H \rightarrow \frac{5}{2}^L$	109.7	12	0.14	2	$(2.1 \pm 0.8) \times 10^{-2}$	0.44×10^{-2}	10.8×10^{-2}	8.5×10^{-2}	20×10^{-2}	$(9.2 \pm 3.7) \times 10^{-3}$	28×10^{-3}	23×10^{-3}
$\frac{5}{2}^H \rightarrow \frac{1}{2}^L$	291.7	100	$E2$		$(8.0 \pm 0.3) \times 10^{-2}$	6.8×10^{-2}	15.8×10^{-2}	14.2×10^{-2}	9.7×10^{-2}			
$\frac{5}{2}^H \rightarrow \frac{3}{2}^L$	245.2	10	0.16[a]	4	$(4.8 \pm 1.4) \times 10^{-4}$	98×10^{-4}	0.000	1.5×10^{-4}	289×10^{-4}	$(7.8 \pm 0.8) \times 10^{-4}$	17.3×10^{-4}	2.7×10^{-4}
$\frac{5}{2}^H \rightarrow \frac{5}{2}^L$	192.6	8.7	0.56[a,b]	5	$(13.0 \pm 2.2) \times 10^{-3}$	2.8×10^{-3}	3.9×10^{-3}	3.5×10^{-3}	47×10^{-3}	$(1.08 \pm 0.22) \times 10^{-3}$	2.62×10^{-3}	1.32×10^{-3}
$\frac{5}{2}^H \rightarrow \frac{7}{2}^L$	84.5	33	0.15	1	$(2.81 \pm 0.39) \times 10^{-1}$	1.12×10^{-1}	2.94×10^{-1}	2.36×10^{-1}	2.47×10^{-1}	$(6.3 \pm 0.9) \times 10^{-2}$	13.2×10^{-2}	12.2×10^{-2}
$\frac{5}{2}^H \rightarrow \frac{3}{2}^H$	82.9	11	0.63	3	1.34 ± 0.13	1.42	1.99	1.88	1.95	$(1.63 \pm 0.18) \times 10^{-2}$	2.68×10^{-2}	1.52×10^{-2}

[a] From Coulomb excitation.

[b] From Krane *et al.*, Phys. Rev. C 7, 263 (1973).

excitation using the semiclassical $E2$ coupled-channels code of Winther and de Boer. Total experimental yields for excitation of the $\frac{9}{2}^L$ and $\frac{7}{2}^H$ states are also consistent with the yields from the coupled-channels code calculation. Finally, the total experimental yield for excitation of the $\frac{9}{2}^H$ state is consistent with the yield from the coupled-channel code calculation. Both Brockmeier *et al.* and Rowe predict that 96.6% of the transition probability for decay of the $\frac{9}{2}^H$ state is contained in the $\frac{9}{2}^H \rightarrow \frac{5}{2}^H$, $\frac{9}{2}^H \rightarrow \frac{7}{2}^L$, and $\frac{9}{2}^H \rightarrow \frac{5}{2}^L$ transitions which are just the transitions observed in our γ-ray spectra. This is a prediction (not fitted because the transitions for decay of the $\frac{9}{2}^H$ state had not been observed at the time of their analysis).

D. Higher states

A number of low-spin ($J < \frac{5}{2}$) states up to an excitation energy ≈ 2.1 MeV have been observed by the (n,γ) reaction.[18,19] A number of the weak γ-ray yields, obtained from our spectra and given in Table I, are attributed to direct $E2$ excitation of these higher states in ^{183}W. In several instances this conclusion is based on secondary gammas from the (n,γ) reaction. Otherwise, the placement is based on the accurately known energy levels in ^{183}W and accurate γ-ray energies (± 0.15 keV) from our spectra. The measured $B(E2)$ for excitation of these higher states in ^{183}W are summarized in Table II. These $B(E2)$ values are $\leq B(E2)_{\text{s.p.}}$.

IV. CONCLUSIONS

Coulomb excitation of states in the $K=\frac{1}{2}$ and $K=\frac{3}{2}$ bands of ^{183}W has provided information on the reduced transition probabilities for the different decay modes of these states. In particular, the prediction of strong cancellation in the $E2$ transition probabilities for the $\frac{3}{2}^H \rightarrow \frac{1}{2}^L$, $\frac{3}{2}^H \rightarrow \frac{5}{2}^L$, and $\frac{5}{2}^H \rightarrow \frac{5}{2}^L$ transitions from Coriolis interaction calculations between these bands has been verified by the experimental results. The general features of the experimental information, $B(E2)$ and $B(M1)$ values and relative phases of the $E2/M1$ mixtures, are reproduced satisfactorily by the wave functions used in the rotation-particle coupling calculations. In particular, the agreement between the calculated and experimental $E2$ transition probabilities is improved with admixed wave functions in which the sign and magnitude of the Coriolis interaction also accounts for the observed single-nucleon-transfer cross sections. This is not unexpected because these reactions give rather direct evidence on the wave functions of low-lying states in odd-A deformed nuclei.[21] There seems to be no real need to invoke the presence of any $\Delta K=2$ band mixing to fit the absolute transition probabilities. The position of the $\frac{9}{2}^H$ state has been located by the γ-ray spectroscopy measurements from multiple $E2$ Coulomb excitation.

This paper was done under the operation of the Union Carbide Corporation under the U.S. Department of Energy Contract No. W-7405-eng-26.

[1] F. S. Stephens, Rev. Mod. Phys. 47, 43 (1975).
[2] J. J. Murray, F. Boehm, P. Marrier, and J. W. M. DuMond, Phys. Rev. 97, 1007 (1955).
[3] A. K. Kerman, Mat. Fys. Medd. Dan. Vid. Selsk. 30, No. 15 (1956).
[4] W. F. Edwards, F. Boehm, J. Rogers, and E. J. Seppi, Nucl. Phys. 63, 97 (1965).
[5] U. Bruber, R. Koch, B. P. Maier, O. W. B. Schult, Z. Naturforsch. 20a, 929 (1965).
[6] D. J. Rowe, Nucl. Phys. 61, 1 (1965).
[7] R. T. Brockmeier, S. Wahlborn, E. J. Seppi, and F. Boehm, Nucl. Phys. 63, 102 (1965).
[8] F. K. McGowan, W. T. Milner, R. O. Sayer, R. L. Robinson, and P. H. Stelson, Nucl. Phys. A289, 253 (1977).
[9] P. H. Stelson and F. K. McGowan, Phys. Rev. 110, 489 (1958).
[10] F. K. McGowan and P. H. Stelson, *Nuclear Spectroscopy and Reactions*, edited by J. Cerny (Academic, New York, 1974), part C, p. 3.
[11] C. E. Bemis, Jr., F. K. McGowan, J. L. C. Ford, Jr., W. T. Milner, P. H. Stelson, and R. L. Robinson, Phys. Rev. C 8, 1466 (1973).
[12] Agda Artna-Cohen, Nucl. Data Sheets 16, 267 (1975).
[13] A. Winther and J. de Boer, in *Coulomb Excitation*, edited by K. Alder and A. Winther (Academic, New York, 1966), p. 303.
[14] O. Hansen, M. C. Olesen, O. Skilbreid, and B. Elbek, Nucl. Phys. 25, 634 (1961).
[15] R. G. Stokstad and B. Persson, Phys. Rev. 170, 1072 (1968).
[16] K. S. Krane, At. Data Nucl. Data Tables 18, 137 (1976).
[17] K. S. Krane, C. E. Olsen, and W. A. Steyert, Phys. Rev. C 7, 263 (1973).
[18] R. F. Casten and W. R. Kane, Phys. Rev. C 7, 419 (1973).
[19] M. L. Stelts, R. E. Chrien, and C. W. Reich, Bull. Am. Phys. Soc. 23, 91 (1978) and private communications.
[20] R. F. Casten, P. Kleinheinz, P. J. Daly, and B. Elbek, Mat. Fys. Medd. Dan. Vid. Selsk. 38, No. 13 (1972).
[21] M. E. Bunker and C. W. Reich, Rev. Mod. Phys. 43, 348 (1971).